Bioorganic & Medicinal Chemistry Letters 29 (2019) 2695–2699

Contents lists available at ScienceDirect

Bioorganic & Medicinal Chemistry Letters

journal homepage: www.elsevier.com/locate/bmcl

Anti-tubercular activity of novel 4-anilinoquinolines and 4-anilinoquinazolines

Christopher R.M. Asquith[a,b], Neil Fleck[c], Chad D. Torrice[d], Daniel J. Crona[d,e], Christoph Grundner[c,f,*], William J. Zuercher[b,e,*]

[a] Department of Pharmacology, School of Medicine, University of North Carolina at Chapel Hill, Chapel Hill, NC 27599, USA
[b] Structural Genomics Consortium, UNC Eshelman School of Pharmacy, University of North Carolina at Chapel Hill, Chapel Hill, NC 27599, USA
[c] Seattle Children's Research Institute, Seattle, WA 98109, USA
[d] Division of Pharmacotherapy and Experimental Therapeutics, UNC Eshelman School of Pharmacy, University of North Carolina at Chapel Hill, Chapel Hill, NC 27599, USA
[e] Lineberger Comprehensive Cancer Center, University of North Carolina at Chapel Hill, Chapel Hill, NC 27599, USA
[f] Department of Global Health, University of Washington, Seattle, WA 98195, USA

ARTICLE INFO

Keywords:
Anti-tubercular
4-Anilinoquinoline
4-Anilinoquinazoline
Mycobacterium tuberculosis (*Mtb*)

ABSTRACT

We screened a series of 4-anilinoquinolines and 4-anilinoquinazolines and identified novel inhibitors of *Mycobacterium tuberculosis* (*Mtb*). The focused 4-anilinoquinoline/quinazoline scaffold arrays yielded compounds with high potency and the identification of 6,7-dimethoxy-*N*-(4-((4-methylbenzyl)oxy)phenyl)quinolin-4-amine (**34**) with an MIC_{90} value of 0.63–1.25 μM. We also defined a series of key structural features, including the benzyloxy aniline and the 6,7-dimethoxy quinoline ring, that are important for *Mtb* inhibition. Importantly the compounds showed very limited toxicity and scope for further improvement by iterative medicinal chemistry.

Mycobacterium tuberculosis (*Mtb*), the causative agent of tuberculosis (TB) in humans,[1] infects nearly a third of the earth's population and caused 1.6 million worldwide deaths in 2017.[2] With nearly ten million new cases of active disease each year, TB is now the leading cause of death from infectious disease globally.[2] Current therapeutic strategies involve the use of a combination of anti-microbial agents including ethambutol, isoniazid, pyrazinamide and rifampicin (Fig. 1).[3] However, > 5% of *Mtb* infections now involve multidrug-resistant (MDR-TB) and extensively drug-resistant (XDR-TB) *Mtb* strains. MDR-TB is associated with a 50% mortality rate whereas XDR-TB is nearly always fatal.[4] There is an urgent need for new therapeutic strategies.

Human protein kinases are pharmacologically tractable enzymes targeted by more than three dozen approved medicines.[5] Hundreds of additional kinase inhibitors are under clinical and preclinical investigation. There is growing recognition that pathogen kinases may be targeted in the treatment of infectious diseases.[6,7] Considering the conserved ATP-binding site across species, we looked to screen collections of ATP-competitive inhibitors of human kinases for their anti-tubercular activity.

To identify new chemical starting points against *Mtb* we looked to lapatinib, gefitinib, and erlotinib as starting points which have recently been revealed to have activity against *Mtb* (Fig. 2.).[5,8] We tested the activity of lapatinib, gefitinib, and erlotinib against *Mtb* by measuring luminescence and growth on solid medium across a series of four two-fold dilutions starting at 20 μM (Table 1).[9,10] The reduction of visible growth on solid medium demonstrated the compounds to be bactericidal.

Gefitinib treatment had no effect relative to the absence of compound. Erlotinib induced a modest effect that appeared to plateau at a signal of approximately 70%. In contrast, lapatinib showed activity even at 5 μM and reduced the relative *Mtb* signal to below 10% at 20 μM. This result suggested that the 4-benzyloxy aniline substituent might be important for anti-*Mtb* activity. These compounds demonstrate only limited toxicity in a human skin fibroblast cell line (WS-1) counter screen.[11]

To further explore quinazoline *Mtb* activity, we profiled several focused arrays of compounds to probe the structure activity relationships of the quinoline/quinazoline. We hence synthesized a series of compounds (**1–34**) following up on the results listed in Table 1, exploring the 4-anilinoquinoline and 4-anilinoquinazoline scaffolds through nucleophilic aromatic displacement of 4-chloroquin(az)olines (Scheme 1). We were able to access products in good to excellent yields (55–91 %) consistent with previous reports and without protection of the alcohol substituted quin(az)oline starting material.[11–13]

The first set of compounds probed a replacement of the 6-postion

* Corresponding authors at: Seattle Children's Research Institute, Seattle, WA 98109, USA (C. Grundner). Structural Genomics Consortium, UNC Eshelman School of Pharmacy, University of North Carolina at Chapel Hill, Chapel Hill, NC 27599, USA (W. J. Zuercher).
E-mail addresses: Christoph.Grundner@seattlechildrens.org (C. Grundner), william.zuercher@unc.edu (W.J. Zuercher).

https://doi.org/10.1016/j.bmcl.2019.07.012
Received 18 June 2019; Accepted 5 July 2019
Available online 10 July 2019
0960-894X/

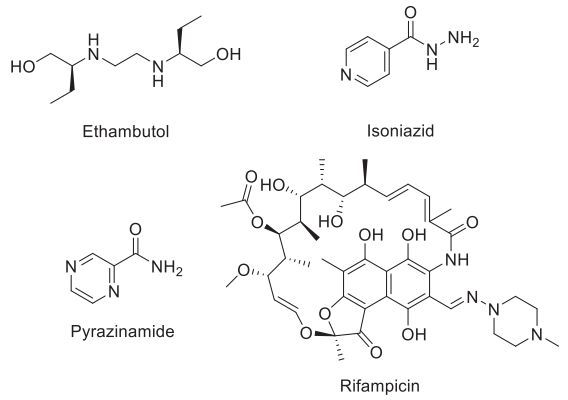

Figure 1. Current therapeutics for treatment of *Mycobacterium tuberculosis* infections.

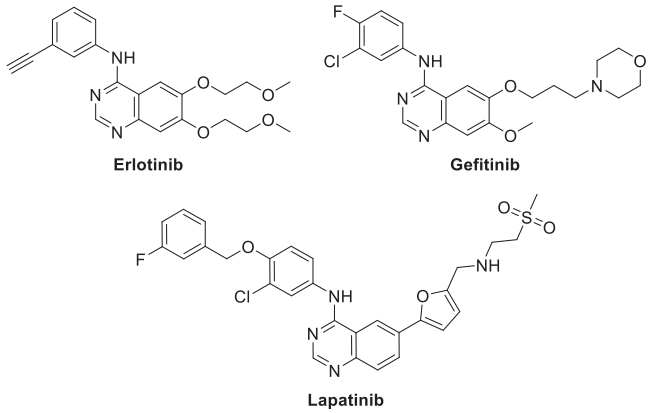

Figure 2. Structures of clinical quinazolines.

Table 1
Results of clinical inhibitors.

Compound	*Mtb* signal[a]					WS-1[b]
/μM	1.25	2.5	5	10	20	(μM)
Gefitinib	1.08	1.09	1.05	1.08	1.05	23
Erlotinib	1.05	0.96	0.90	0.68	0.70	8.6
Lapatinib	0.99	0.90	0.74	0.17	0.08	13

[a] Relative luminescence measured at 3 days after treatment. Values = RLU (sample)/RLU(no compound) at μM concentrations and no effect at 0.625 μM; [b]ref[11]

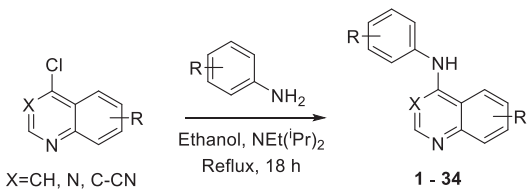

Scheme 1. General synthetic procedure.

morpholine segment of gefitinib with a simple alcohol on the lapatinib scaffold (Table 2).[14] Although neither the 6-OH (**1**) or 7-OH (**2**) quinazoline showed appreciable activity, the 6,7-dihydroxy compound (**3**) began to inhibit *Mtb* growth at higher concentrations. The analogous set of methoxy-substituted compounds (**4–6**) had very similar activity profiles. The 6-OH quinoline (**7**) showed improved activity relative to the matched quinazoline (**1**). The inclusion of fluorine substitution on the phenyl ring distal to the quinazoline (**8–10**) led to markedly increased activity for all three isomers. At 20 μM, **8–10** all reduced

Table 2
Results of alcohol replacement of lapatinib and gefitinib (**1–12**).

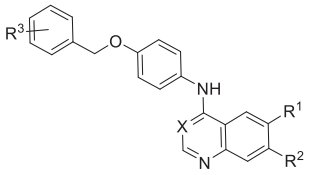

Compound	X	R^1	R^2	R^3	*Mtb* signal[a] (μM)					WS-1[b]
					1.25	2.5	5	10	20	(μM)
1	N	OH	H	H	0.95	0.94	0.96	0.90	0.80	26
2	N	H	OH	H	0.90	0.90	0.89	0.88	0.89	> 100
3	N	OH	OH	H	0.95	0.93	0.91	0.76	0.69	8.8
4	N	OMe	H	H	1.04	1.07	0.89	0.83	0.62	> 100
5	N	H	OMe	H	1.05	1.12	0.99	0.87	0.64	> 100
6	N	OMe	OMe	H	1.04	1.04	0.83	0.77	0.60	> 100
7	CH	OH	H	H	0.95	0.86	0.66	0.42	0.37	2.5
8	N	OH	H	4-F	0.86	0.76	0.64	0.44	0.32	> 100
9	N	OH	H	3-F	0.76	0.64	0.49	0.39	0.25	12
10	N	OH	H	2-F	0.89	0.82	0.63	0.46	0.28	28
11	N	H	OH	4-F	0.94	1.01	0.90	0.89	0.83	> 100
12	N	OH	OH	4-F	1.04	1.14	1.00	0.89	0.76	> 100

[a] Relative luminescence measured at 3 days after treatment. Values = RLU (sample)/RLU(no compound) at μM concentrations and no effect at 0.625 μM; [b]IC_{50} (mean average n = 4), 48 h

the relative *Mtb* signal to 25–37 %, and a modest but discernable reduction in signal was observed at 1.25 μM. Interestingly, the effect of fluorine substitution led to a different activity pattern from changing quinazoline ring substitution as the modification of **1** to the 7-OH (**11**) or 6,7-$(OH)_2$ (**12**) resulted in a significant loss of activity, even at 20 μM. These results demonstrated that *Mtb* activity was sensitive to changes at multiple parts of the template and that these changes were not necessarily additive. We counter screened **1–12** in human skin fibroblast cells (WS-1) and observed very limited toxicity with **3** and **7** the only compounds in the single digit micromolar range (IC_{50} = 8.8 and 2.5 μM respectively).[15]

The next set of quin(az)olines profiled was prepared to explore the contributions from both the aniline and the core heterocycle (Table 3).[11,16] The larger 3,4,5-trimethoxyphenyl aniline was employed on several diversely substituted quinolines and quinazolines (**13–18**) which led to no observable activity except when paired with the 6,7-$(OCH_2CH_2OMe)_2$-quinazoline of erlotinib (**19**) which had only slight activity at 20 μM. On the other hand, incorporation of the aniline fragment from erlotinib (3-ethynylphenyl) did yield several active compounds, including the quinoline analog of erlotinib (**20**). The erlotinib aniline with a 6,7-$(OMe)_2$-substituted quinoline core (**21**) or quinazoline (**22**) showed activity but not with the 3-cyanoquinoline (**23**). The analogous 3-bromophenyl aniline compounds (**24–26**) showed higher activity than the paired 3-ethynylphenyl compounds. Finally, the aniline substitution from lapatinib (3-Cl-4-(2-F-PhO)Ph) yielded a marginally active quinazoline (**27**) and a highly active quinoline (**28**) that had 10% *Mtb* signal at 20 μM. We counter screened **13–28** in WS-1 cells and observed limited toxicity in most compounds. However, the bromine substitution appeared to increase toxicity (**24–26**) along with the lapatinib derivatives (**27–28**).

A subsequent set of compounds explored features of the 4-benzyloxyaniline portion of the quinoline template (Table 4).[17,18] Variation of the ether linkage to an amide and addition of a hydroxy on the aniline portion revealed an activity pattern where 6,7-dimethoxy substitution with the benzylic arm was active (**29–30**). In contrast, truncation of the benzyl also removed the activity as in acetamide **31,** which had no effect on *Mtb*. The 6-methoxy (**32**) and 7-methoxy (**33**) showed no reduction in *Mtb* signal at 20 μM. However, switching back

Table 3
Matched pair comparison of structures similar to erlotinib and lapatinib (**13–28**).

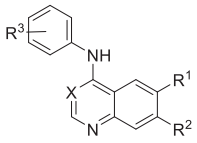

Compound	R^1	R^2	X	R^3	*Mtb* signal[a,b]			WS-1[c]
					5 μM	10 μM	20 μM	(μM)
13	CF_3	H	CH	3,4,5-$(OMe)_3$	1.23	1.14	1.21	> 100
14	CF_3	H	N	3,4,5-$(OMe)_3$	1.25	1.12	1.06	> 100
15	Br	H	CH	3,4,5-$(OMe)_3$	1.35	1.41	1.28	> 100
16	OMe	OMe	CH	3,4,5-$(OMe)_3$	1.26	1.11	1.06	> 100
17	OMe	OMe	N	3,4,5-$(OMe)_3$	1.03	1.01	0.94	> 100
18	OMe	OMe	C-CN	3,4,5-$(OMe)_3$	1.03	1.01	0.97	> 100
19	6,7-$(OCH_2CH_2OMe)_2$		N	3,4,5-$(OMe)_3$	1.02	0.96	0.87	> 100
20	6,7-$(OCH_2CH_2OMe)_2$		CH	3-Ethynyl	0.88	0.79	0.58	> 100
21	OMe	OMe	CH	3-Ethynyl	1.02	0.89	0.67	> 100
22	OMe	OMe	N	3-Ethynyl	0.93	0.83	0.69	> 100
23	OMe	OMe	C-CN	3-Ethynyl	1.08	1.03	0.98	> 100
24	OMe	OMe	CH	3-Bromo	1.03	0.90	0.60	9.6
25	OMe	OMe	N	3-Bromo	0.98	0.71	0.65	3.9
26	OMe	OMe	C-CN	3-Bromo	0.88	0.56	0.37	11
27	OMe	OMe	N	3-Cl-4-(OBn-3-F)	0.92	0.74	0.80	1.1
28	OMe	OMe	CH	3-Cl-4-(OBn-3-F)	0.78	0.22	0.10	11

[a] Relative luminescence was measured at 3 days after treatment. Values = RLU(sample)/RLU(no compound); [b]None of the compounds reduced the relative *Mtb* signal below 95% at 1.3 or 2.5 μM; [c]IC_{50} (mean average n = 4), 48 h

Table 4
Matched pair comparison of benzyloxyaniline.

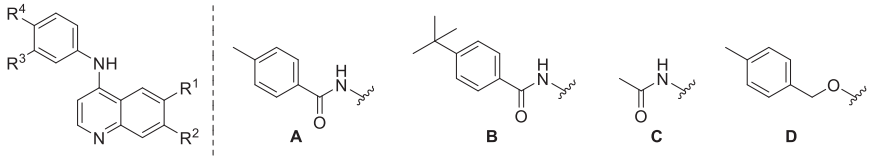

Compound	R^1	R^2	R^3	R^4	*Mtb* signal[a] (μM)					WS-1[b]
					1.25	2.5	5	10	20	(μM)
29	OMe	OMe	OH	**A**	1.14	1.09	1.13	1.05	0.45	16
30	OMe	OMe	OH	**B**	1.10	1.12	1.06	0.72	0.25	2.6
31	OMe	OMe	H	**C**	1.21	1.10	1.11	1.07	1.02	9.7
32	OMe	H	OH	**A**	1.11	1.17	1.14	1.28	0.95	10
33	H	OMe	OH	**A**	1.13	1.11	1.09	1.11	0.96	4.7
34	OMe	OMe	H	**D**	0.43	0.17	0.10	0.08	0.09	5.4

[a] Relative luminescence was measured at 3 days after treatment. Values = RLU(sample)/RLU(no compound).
[b] IC_{50} (mean average n = 4), 48 h.

to the 4-methyl benzyl ether linked compound **34** yielded the most potent activity observed with any compound in the present study, with a robust signal observed even at 1.25 μM. The *Mtb* MIC_{90} for **34** was in the 0.63–1.25 μM range. However, the kill curve plateaued at 5 μM, and no improved killing was observed at higher doses (98 % inhibition at 5 μM; 98 % inhibition at 20 μM) (Fig. 3).

As with the other compound sets, we evaluated **29–34** in human skin fibroblast cells (WS-1) and observed moderate toxicity in the single digit micromolar range for most compounds.[18] Importantly, the anti-*Mtb* effects of compounds appeared to be divergent from the toxic effects in WS-1 cells, suggesting that the *Mtb* effects were not driven by nonspecific cytotoxicity. The most potent anti-*Mtb* compound **34** had WS-1 IC_{50} = 5.4 μM, substantially higher than its *Mtb* MIC_{90} value and within threefold of the IC_{50} values for erlotinib and lapatinib. This result demonstrated that, in the human WS-1 cell line, **34** behaved comparably to two approved medicines.

These structure activity relationships between *Mtb* activity and the 4-anilinoquinoline/quinazoline scaffold have the potential to inform a medicinal chemistry strategy for enhanced *Mtb* activity. The most sensitive structural changes were found to be in the ring appended to the aniline rather than in the quin(az)oline core.

This body of work provides a number of exciting starting points for further optimization, with limited non-specific toxicity. However, the failure to achieve complete bacterial killing led us to deprioritize the series due to the potential for resistance to develop. The mechanism of anti-*Mtb* activity of the quin(az)olines has yet to be defined. These

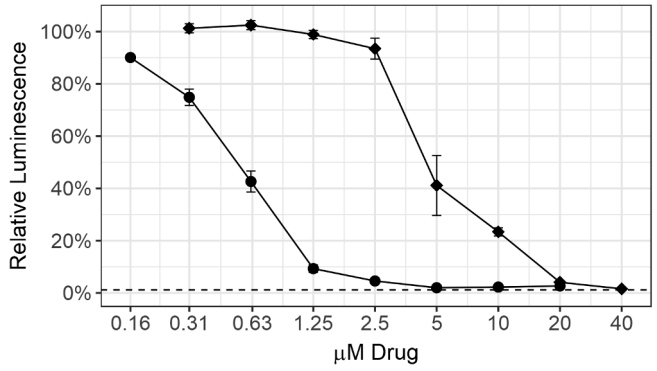

Figure 3. MIC determination by two different assays for **34** (circle) and lapatanib (diamond). Data points represent the mean of 3 biological replicates with standard deviation. The dashed line labeled 1 % inoculum represents an inoculation of 1 % of the number of cells used for compound testing. This control was used to determine 99 % inhibition of growth.

compounds were originally prepared as inhibitors of human kinases targeting the ATP-binding site, arational starting hypothesis for the mechanism of action is that the effects of these compounds are mediated by inhibition of *Mtb* kinases. However, it is possible that the observed phenotypes may originate from modulation of other, non-kinase ATP-binding proteins in the organism.

Gefitinib, erlotinib, and lapatinib have previously been reported to inhibit the intracellular growth of *Mtb*. Multiple lines of evidence were described suggesting inhibition of the host target epidermal growth factor receptor (EGFR) was responsible for this activity.[15] However our results demonstrate that proteins within the pathogen itself may be targeted as well. The benzyl substituent present in the molecule showed a pivotal effect to potency, as is highlighted by the enhanced activity of **34** relative to **30**. The present results help define a de-risked medicinal chemistry trajectory towards anti-tubercular compounds with targets in both the host and the parasite itself. Such dual acting compounds might offer advantages in efficacy and/or reduction in propensity for resistance.

Acknowledgments

The SGC is a registered charity (number 1097737) that receives funds from AbbVie, Bayer Pharma AG, Boehringer Ingelheim, Canada Foundation for Innovation, Eshelman Institute for Innovation, Genome Canada, Innovative Medi-cines Initiative (EU/EFPIA) [ULTRA-DD grant no. 115766], Janssen, Merck KGaA Darmstadt Germany, MSD, Novartis Pharma AG, Ontario Ministry of Economic Development and Innovation, Pfizer, São Paulo Research Foundation-FAPESP, Takeda, and Wellcome [106169/ZZ14/Z]. C. G. is supported by R01 AI117023 from the NIH/NIAID. We are grateful Dr. Brandie Ehrmann for LC-MS/HRMS support provided by the Mass Spectrometry Core Laboratory at the University of North Carolina at Chapel Hill.

Appendix A. Supplementary data

Supplementary data to this article can be found online at https://doi.org/10.1016/j.bmcl.2019.07.012.

References

1. Pai M, Behr MA, Dowdy D, et al. *Nat Rev Dis Primers.* 2016;2:16076.
2. World Health Organization. Global Tuberculosis Report 2018 (WHO, 2018).
3. Chan ED, Iseman MD. *BMJ.* 2002;325:1282.
4. Floyd K, Glaziou P, Zumla A, Raviglione M. *Lancet Respir Med.* 2018;6:299.
5. Ferguson FM, Gray NS. *Nat Rev Drug Discov.* 2018;17:353.
6. Sachan M, Srivastava A, Ranjan R, Gupta A, Pandya S, Misra A. *Curr Pharm Des.* 2016;22:2599.
7. Glennon EKK, Dankwa S, Smith JD, Kaushansky A. *Trends Parasitol.* 2018;34:843.
8. Stanley SA, Barczak AK, Silvis MR, et al. *PLoS Pathog.* 2014;10:e1003946.
9. Andreu N, Fletcher T, Krishnan N, Wiles S, Robertson BD. *J Antimicrob Chemother.* 2012;67:404.
10. An H37Rv strain containing an auto-luminescence operon (LuxABCDE) was grown to log phase, diluted and re-grown for at least 2 doublings to a final OD600 of 0.005. Cultures were dispensed into 96-well white, flat-bottom plates in 100 μL final volume. Luminescence was quantified using a PHERTAstar plate reader (BMG Labtech) blanked against 7H9 media.
11. Asquith CRM, Naegeli KM, East MP, et al. *J Med Chem.* 2019;62:4772.
12. Asquith CRM, Laitinen T, Bennett JM, et al. *ChemMedChem.* 2018;13:48.
13. Asquith CRM, Treiber DK, Zuercher WJ. *Bioorg Med Chem Lett.* 2019;29:1727.
14.. General procedure for the synthesis of 4-anilinoquin(az)olines: 4-chloroquin(az)oline derivative (1.0 eq.), aniline derivative (1.1 eq.), and $^{i}Pr_2NEt$ (2.5 eq.) were suspended in ethanol (10 mL) and refluxed for 18 h. The crude mixture was purified by flash chromatography using EtOAc:hexane followed by 1-5 % methanol in EtOAc; After solvent removal under reduced pressure, the product was obtained as a free following solid or recrystallized from ethanol/water. **4-{ [4-(benzyloxy)phenyl] amino}quinazolin-6-ol** (**1**) as a yellow solid (68 %, 220 mg, 0.640 mmol) MP 231-233 °C; ^{1}H NMR (400 MHz, DMSO-d_6) δ 11.21 (s, 1H), 10.91 (s, 1H), 8.75 (s, 1H), 8.04 (d, J = 2.5 Hz, 1H), 7.88 (d, J = 9.0 Hz, 1H), 7.70 (dd, J = 9.1, 2.5 Hz, 1H), 7.62 – 7.57 (m, 2H), 7.52 – 7.44 (m, 2H), 7.44 – 7.37 (m, 2H), 7.37 – 7.30 (m, 1H), 7.14 – 7.09 (m, 2H), 5.16 (s, 2H). ^{13}C NMR (101 MHz, DMSO-d_6) δ 158.8, 157.8, 156.7, 148.1, 136.9, 131.6, 129.7, 128.5 (2C, s), 127.9, 127.7 (2C, s), 126.5, 126.2 (2C, s), 121.2, 114.92, 114.85 (2C, s), 107.1, 69.4. HRMS m/z $[M+H]^+$ calcd for $C_{21}H_{18}N_3O_2$: 344.1399 found = 344.1386; LC t_R = 4.24 min, > 98 % Purity. **4-{ [4-(benzyloxy)phenyl] amino}quinazolin-7-ol** (**2**) as a light yellow solid (78 %, 223 mg, 0.648 mmol) MP 277-279 °C; ^{1}H NMR (400 MHz, DMSO-d_6) δ 11.76 (s, 1H), 11.42 (s, 1H), 8.76 (d, J = 9.0 Hz, 1H), 8.74 (s, 1H), 7.59 – 7.54 (m, 2H), 7.49 – 7.44 (m, 2H), 7.42 – 7.38 (m, 2H), 7.36 – 7.28 (m, 3H), 7.12 – 7.07 (m, 2H), 5.15 (s, 2H). ^{13}C NMR (101 MHz, DMSO-d_6) δ 164.3, 158.9, 156.6, 150.5, 140.4, 136.9, 129.7, 128.5 (2C, s), 127.9, 127.7 (2C, s), 127.1, 126.3 (2C, s), 119.4, 114.8 (2C, s), 105.8, 102.0, 69.4. HRMS m/z $[M+H]^+$ calcd for $C_{21}H_{18}N_3O_2$: 344.1399 found = 344.1386; LC t_R = 4.33 min, > 98 % Purity. **4-{ [4-(benzyloxy)phenyl] amino}quinazoline-6,7-diol** (**3**) as a light yellow solid (69 %, 189 mg, 0.527 mmol) MP 272-274 °C; ^{1}H NMR (400 MHz, DMSO-d_6) δ 10.32 (s, 2H), 8.53 (s, 1H), 7.91 (s, 1H), 7.64 – 7.53 (m, 2H), 7.50 – 7.44 (m, 2H), 7.43 – 7.37 (m, 2H), 7.36 – 7.30 (m, 2H), 7.20 (s, 1H), 7.10 – 7.01 (m, 2H), 5.13 (s, 2H). ^{13}C NMR (101 MHz, DMSO-d_6) δ 157.4, 155.7, 154.3, 149.1, 147.7, 137.1, 131.2, 128.5 (2C, s), 127.8, 127.7 (2C, s), 125.4 (2C, s), 114.7 (2C, s), 107.3, 106.7, 104.9, 69.4. HRMS m/z $[M+H]^+$ calcd for $C_{21}H_{18}N_3O_3$: 360.1348 found = 360.1335; LC t_R = 4.22 min, > 98 % Purity. ***N*-(4-(benzyloxy)phenyl)-6-methoxyquinazolin-4-amine** (**4**) as a light yellow solid (84 %, 231 mg, 0.647 mmol) MP 270-272 °C; ^{1}H NMR (400 MHz, DMSO-d_6) δ 11.64 (s, 1H), 8.79 (s, 1H), 8.41 (d, J = 2.6 Hz, 1H), 7.92 (d, J = 9.1 Hz, 1H), 7.72 (dd, J = 9.2, 2.5 Hz, 1H), 7.68 – 7.53 (m, 2H), 7.53 – 7.18 (m, 5H), 7.18 – 7.04 (m, 2H), 5.17 (s, 2H), 4.00 (s, 3H). ^{13}C NMR (101 MHz, DMSO-d_6) δ 159.0 (2C, s), 156.8, 148.8, 136.9, 133.3, 129.6, 128.5 (2C, s), 127.9, 127.7 (2C, s), 126.8, 126.4 (2C, s), 121.4, 114.9 (2C, s), 114.6, 104.6, 69.4, 56.7. HRMS m/z $[M+H]^+$ calcd for $C_{22}H_{19}N_3O_2$: 357.1477 found = 358.1546; LC t_R = 4.53 min, > 98 % Purity. ***N*-[4-(benzyloxy)phenyl] -7-methoxyquinazolin-4-amine** (**5**) as a colourless solid (91 %, 251 mg, 0.701 mmol) MP 247-249 °C; ^{1}H NMR (400 MHz, DMSO-d_6) δ 11.58 (s, 1H), 8.87 (d, J = 9.3 Hz, 1H), 8.81 (s, 1H), 7.71 – 7.57 (m, 2H), 7.58 – 7.12 (m, 7H), 7.13 – 6.99 (m, 2H), 5.15 (s, 2H), 3.97 (s, 3H). ^{13}C NMR (101 MHz, DMSO-d_6) δ 164.7, 158.9, 156.7, 150.8, 140.7, 136.9, 129.6, 128.5 (2C, s), 127.9, 127.7 (2C, s), 127.0, 126.3 (2C, s), 118.7, 114.8 (2C, s), 107.1, 100.1, 69.4, 56.3. HRMS m/z $[M+H]^+$ calcd for $C_{22}H_{19}N_3O_2$: 357.1477 found = 358.1547; LC t_R = 4.49 min, > 98 % Purity. ***N*-(4-(benzyloxy)phenyl)-6,7-dimethoxyquinazolin-4-amine** (**6**) as a colourless solid (84 %, 217 mg, 0.561 mmol) MP 250-252 °C; ^{1}H NMR (400 MHz, DMSO-d_6) δ 11.44 (s, 1H), 8.73 (s, 1H), 8.36 (s, 1H), 7.68 – 7.56 (m, 2H), 7.55 – 7.43 (m, 2H), 7.43 – 7.15 (m, 4H), 7.15 – 7.03 (m, 2H), 5.15 (s, 2H), 4.00 (s, 3H), 3.96 (s, 3H). ^{13}C NMR (101 MHz, DMSO-d_6) δ 157.9, 156.5, 156.0, 150.0, 148.6, 137.0, 135.5, 129.9, 128.5 (2C, s), 127.9, 127.7 (2C, s), 126.3 (2C, s), 114.8 (2C, s), 107.1, 104.1, 99.8, 69.4, 57.0, 56.4. HRMS m/z $[M+H]^+$ calcd for $C_{23}H_{21}N_3O_3$: 388.1661 found = 388.1651; LC t_R = 4.55 min, > 98 % Purity. **4-{ [4-(benzyloxy)phenyl] amino}quinolin-6-ol** (**7**) as a light yellow solid (64 %, 182 mg, 0.532 mmol) MP 218-220 °C; ^{1}H NMR (400 MHz, DMSO-d_6) δ 10.67 (s, 1H), 10.37 (s, 1H), 8.32 (d, J = 6.8 Hz, 1H), 7.96 (d, J = 9.1 Hz, 1H), 7.91 (d, J = 2.5 Hz, 1H), 7.63 (dd, J = 9.1, 2.4 Hz, 1H), 7.58 – 7.44 (m, 2H), 7.46 – 7.22 (m, 5H), 7.23 – 7.13 (m, 2H), 6.57 (d, J = 6.8 Hz, 1H), 5.17 (s, 2H). ^{13}C NMR (101 MHz, DMSO-d_6) δ 157.3, 156.5, 154.1, 140.1, 136.8, 132.2, 130.2, 128.5 (2C, s), 128.0, 127.8 (2C, s), 127.2 (2C, s), 124.9, 121.9, 118.7, 116.0 (2C, s), 105.4, 98.6, 69.5. HRMS m/z $[M+H]^+$ calcd for $C_{22}H_{19}N_2O_2$: 343.1447 found = 343.1433; LC t_R = 4.45 min, > 98 % Purity. **4-({4-[(4-fluorophenyl)methoxy] phenyl}amino)quinazolin-6-ol** (**8**) as a yellow solid (76 %, 228 mg, 0.631 mmol) Decomposed > 200 °C; ^{1}H NMR (400 MHz, DMSO-d_6) δ 11.22 (s, 1H), 10.91 (s, 1H), 8.75 (s, 1H), 8.05 (d, J = 2.5 Hz, 1H), 7.88 (d, J = 9.0 Hz, 1H), 7.70 (dd, J = 9.0, 2.4 Hz, 1H), 7.67 – 7.54 (m, 2H), 7.57 – 7.39 (m, 2H), 7.40 – 7.17 (m, 2H), 7.17 – 7.01 (m, 2H), 5.14 (s, 2H). ^{13}C NMR (101 MHz, DMSO-d_6) δ 163.0, 159.7 (d, J = 175.5 Hz), 157.8, 156.6, 148.1, 133.2 (d, J = 3.0 Hz), 131.6, 130.0 (d, J = 8.3 Hz, 2C), 129.8, 126.5, 126.2 (2C, s), 121.2 115.3 (d, J = 21.4 Hz, 2C), 114.93, 114.86 (2C, s), 107.1, 68.7. HRMS m/z $[M+H]^+$ calcd for $C_{21}H_{17}N_3O_2F$: 362.1305 found = 362.1290; LC t_R =4.31 min, > 98 % Purity. **4-({4-[(3-fluorophenyl)methoxy] phenyl}amino) quinazolin-6-ol** (**9**) as a dark green solid (58 %, 174 mg, 0.482 mmol) 138-140 °C; ^{1}H NMR (400 MHz, DMSO-d_6) δ 11.25 (s, 1H), 10.94 (s, 1H), 8.74 (s, 1H), 8.06 (d, J = 2.5 Hz, 1H), 7.89 (d, J = 9.0 Hz, 1H), 7.71 (dd, J = 9.0, 2.4 Hz, 1H), 7.67 – 7.49 (m, 2H), 7.45 (td, J = 8.0, 6.0 Hz, 1H), 7.41 – 7.22 (m, 2H), 7.21 – 6.93 (m, 3H), 5.19 (s, 2H). ^{13}C NMR (101 MHz, DMSO-d_6) δ 162.2 (d, J = 243.7 Hz), 158.8, 157.8, 156.4, 148.1, 139.9 (d, J = 7.4 Hz), 131.6, 130.5 (d, J = 8.4 Hz), 129.9, 126.5, 126.3 (2C, s), 123.5 (d, J = 2.8 Hz), 121.1, 114.9, 114.9 (2C, s) , 114.6 (d, J = 20.9 Hz), 114.2 (d, J = 21.9 Hz), 107.1, 68.6 (d, J = 1.9 Hz). HRMS m/z $[M+H]^+$ calcd for $C_{21}H_{17}N_3O_2F$: 362.1305 found = 362.1296; LC t_R = 4.25 min, > 98 % Purity. **4-({4-[(2-fluorophenyl)methoxy] phenyl}amino)quinazolin-6-ol** (**10**) as a dark green solid (69 %, 207 mg, 0.573 mmol) 235-237 °C; ^{1}H NMR (400 MHz, DMSO-d_6) δ 11.23 (s, 1H), 10.91 (s, 1H), 8.75 (s, 1H), 8.05 (d, J = 2.5 Hz, 1H), 7.88 (d, J = 9.0 Hz, 1H), 7.70 (dd, J = 9.0, 2.4 Hz, 1H), 7.66 – 7.48 (m, 3H), 7.48 – 7.38 (m, 1H), 7.38 – 7.19 (m, 2H), 7.19 – 7.05 (m, 2H), 5.19 (s, 2H).

^{13}C NMR (101 MHz, DMSO-d_6) 160.4 (d, J = 246.1 Hz), 158.8, 157.8, 156.5, 148.1, 131.7, 130.7 (d, J = 4.1 Hz), 130.5 (d, J = 8.3 Hz), 129.9, 126.5, 126.3 (2C, s), 124.6 (d, J = 3.5 Hz), 123.7 (d, J = 14.5 Hz), 121.2, 115.4 (d, J = 21.0 Hz), 114.9, 114.8 (2C, s), 107.1, 63.8 (d, J = 3.7 Hz). HRMS m/z $[M+H]^+$ calcd for $C_{21}H_{17}N_3O_2F$: 362.1305 found = 362.1291; LC t_R = 4.30 min, > 98 % Purity. **4-((4-((4-fluorobenzyl)oxy)phenyl) amino)quinazolin-7-ol** (**11**) as a grey solid (58 %, 174 mg, 0.482 mmol) Decomposed > 300 °C; ^{1}H NMR (400 MHz, DMSO-d_6) δ 11.74 (s, 1H), 11.38 (s, 1H), 8.81 – 8.66 (m, 2H), 7.66 – 7.38 (m, 4H), 7.29 (dd, J = 6.9, 2.4 Hz, 2H), 7.27 – 7.15 (m, 2H), 7.14 – 7.05 (m, 2H), 5.13 (s, 2H). ^{13}C NMR (101 MHz, DMSO-d_6) δ 164.2, 161.8 (d, J = 243.7 Hz), 158.9, 156.5, 150.5, 140.5, 133.2 (d, J = 3.0 Hz), 130.0 (d, J = 8.3 Hz, 2C), 129.7, 127.1, 126.3 (2C, s), 119.4, 115.3 (d, J = 21.4 Hz, 2C), 114.8 (2C, s), 105.8, 102.1, 68.7. HRMS m/z $[M+H]^+$ calcd for $C_{21}H_{17}N_3O_2F$: 362.1305 found = 362.1291; LC t_R = 4.44 min, > 98 % Purity. **4-((4-((4-fluorobenzyl)oxy)phenyl)amino)quinazoline-6,7-diol** (**12**) as a colourless solid (55 %, 158 mg, 0.420 mmol) 285-290 °C; ^{1}H NMR (400 MHz, DMSO-d_6) δ 10.34 (s, 1H), 8.55 (s, 1H), 7.88 (s, 1H), 7.70 – 7.35 (m, 4H), 7.33 – 7.12 (m, 3H), 7.12 – 7.01 (m, 2H), 5.12 (s, 2H). ^{13}C NMR (126 MHz, DMSO-d_6) δ 161.8 (d, J = 243.5 Hz), 157.4, 155.7, 154.4, 149.0, 147.7, 137.4, 133.3 (d, J = 8.3 Hz, 2C), 130.9, 130.0 (d, J = 8.4 Hz, 2C), 125.4, 115.3 (d, J = 21.3 Hz, 2C), 114.8 (s, 2C), 107.2, 106.8, 104.6, 68.7. HRMS m/z $[M+H]^+$ calcd for $C_{21}H_{17}N_3O_3F$: 378.1254 found = 378.1240; LC t_R = 4.29 min, > 98 % Purity.

15. Toxicity cell assay: WS-1 cells were seeded at 400 cells/well in 384 well plates. Cells were treated with compound at 24 h after plating, and cell viability was assessed at 48 h using alamarBlue (ThermoFisher, USA). Fluorescence was measured using Tecan Infinite 200 PRO plate reader with excitation at 535 nM and emission at 590 nM. IC_{50} values were determined by nonlinear regression using Graphpad Prism™ software.
16. Compounds **13**-**28** prepared as previously described.[11].
17. Compounds **29**-**34** prepared as previously described.[18].
18. Asquith CRM, Maffuid KA, Laitinen T, et al. *bioRxiv*. 2019. https://doi.org/10.1101/545525.